



Liu, X., Jiang, J. Z., Titurus, B., Harrison, A. J. L., & McBryde, D. (2017). Testing and modelling of the damping effects for fluid-based inerters. *Procedia Engineering*, 199, 435-440.
<https://doi.org/10.1016/j.proeng.2017.09.171>

Publisher's PDF, also known as Version of record

License (if available):
CC BY-NC-ND

Link to published version (if available):
[10.1016/j.proeng.2017.09.171](https://doi.org/10.1016/j.proeng.2017.09.171)

[Link to publication record in Explore Bristol Research](#)
PDF-document

This is the final published version of the article (version of record). It first appeared online via Elsevier at <https://doi.org/10.1016/j.proeng.2017.09.171>. Please refer to any applicable terms of use of the publisher.

University of Bristol - Explore Bristol Research

General rights

This document is made available in accordance with publisher policies. Please cite only the published version using the reference above. Full terms of use are available:
<http://www.bristol.ac.uk/pure/about/ebr-terms>



X International Conference on Structural Dynamics, EURODYN 2017

Testing and modelling of the damping effects for fluid-based inerters

Xiaofu Liu^a, Jason Zheng Jiang^{a,*}, Branislav Titurus^b, Andrew J. L. Harrison^a, Daniel McBryde^a

^aDepartment of Mechanical Engineering, University of Bristol, University walk, Bristol BS8 1TR, UK

^bDepartment of Aerospace Engineering, University of Bristol, University walk, Bristol BS8 1TR, UK

Abstract

The inerter is a dynamic physical dual of a capacitor via the force-current analogy, having the property that the force across the terminals is ideally proportional to their relative acceleration. Fluid-based forms of inerter have physical advantages of improved durability, inherent damping and simplicity of design in comparison to mechanical flywheel-based forms. Apart from the inertial effect, linear and nonlinear damping also occur in the helical-tube fluid inerter arrangement. In previous studies, discrepancies between experimental and theoretical results have been found. These are believed to arise from imperfect modelling of damping and pressure losses within the helical tube. To model these effects more accurately, this paper introduces a new experimental set-up. Pressure gauges are used to measure the pressure drop across the helical channel during constant velocity tests. This approach delivers improved agreement between experimental and theoretical results. The sources of minor remaining discrepancies are further analysed. Furthermore, a new fluid-based inerter design is first proposed with different damping characteristics, the theoretical damping comparison is also presented between these two designs.

© 2017 The Authors. Published by Elsevier Ltd.

Peer-review under responsibility of the organizing committee of EURODYN 2017.

Keywords: inerter, fluid, damping, helical-tube, meander-tube, pressure gauge

1. Introduction

The research on inerter have been continuously developed ever since the idea of inerter is first introduced by Smith in 2002 [1]. Different from the mass element, an inerter has the property that the applied force is proportional to the relative acceleration across the two terminals. In terms of the physical realisations of inerter, the flywheel-based design has been extensively studied, including experimental testing [2, 3] and nonlinearity analysis [4]. However, a few unavoidable drawbacks of the flywheel-based design, such as excessive wear of the transmission mechanism, have restricted the application of inerter to be only in the racing industry. Recently, an alternative fluid-base design was introduced in [5] with apparent advantages of durability, structural simplicity and low cost.

According to the results given in [5], the parasitic damping is one of the most critical effects that need to accurately modelled for fluid inerters. Limited work was attempted to test and analyse the nonlinear properties of the helical-tube fluid inerter. There are still significant discrepancies observed between theoretical and experimental damping [5, 6]. In this paper, an experimental set-up consisting of two pressure gauges is used to directly measure the pressure drop across the helical tube channel, such that the parasitic damping can be more accurately tested. A prototype of helical-tube fluid inerter is built for experimental testing. It

* Corresponding author. Tel.: +44 (0) 117 95 45612.

E-mail address: z.jiang@bristol.ac.uk

will be shown that improved agreement of the damping effects between experimental and theoretical values can be obtained. In addition, a new design of meander-tube fluid inerter is introduced, which aims to study the new form of parasitic damping relative to the original helical-tube design, while providing the same level of inertance. The key feature of this new design is to minimise the length of curvature in the external tube. Based on the chosen formula of damping, the theoretical comparison between the damping of meander-tube design and helical-tube design are made to illustrate the differences between the two designs.

This paper is organised as follows. Section 2 introduces the prototype design of helical-tube fluid inerter and corresponding test rig design for this specific prototype. In Section 3, the experimental data are collected and analysed for each triangular wave test, and the theoretical modelling of helical tube damping is carried out based on the experimental results. A new design of fluid inerter namely the meander-tube design, is proposed in Section 4 with its damping characteristics analysed theoretically and compared with the helical-tube fluid inerter. Conclusions are presented in Section 5.

2. Prototype design and experimental setup

Prototype of a helical-tube fluid inerter is built at the University of Bristol, as shown in Fig. 1. This prototype consists of a main cylinder and a separate helical tube coil, which enables different sets of helical tubes with various diameters and bend radiuses to be easily connected for testing. The ball valves between the main cylinder and the helical tube are designed to help partially isolate the fluid in cylinder chambers and in helical tube channel, while filling the chamber with fluid or changing the external tube.

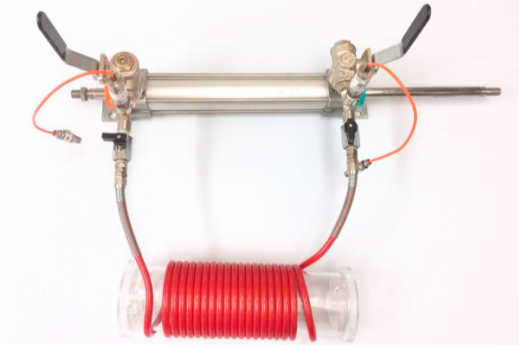


Fig. 1. The helical-tube fluid inerter prototype built in the University of Bristol.

In addition, two built-in pressure gauges (Druck PDCR 812) are used to precisely record the pressure values of the working fluid at the inlet/outlet of the helical tube channel. The parasitic damping caused by the helical tube can be then derived by processing these pressure signals. For future applications, the integrated design could be made instead, which will have the advantage of compactness and symmetry in design. In this paper, all the theoretical and experimental results are based on this helical-tube fluid inerter with parameters listed in Table 1, while water is chosen to be the working fluid.

Table 1. Design parameters of the helical-tube fluid inerter prototype.

Description	Value
Channel area A_2 (m^2)	2.83×10^{-5}
Piston area A_1 (m^2)	1.1×10^{-3}
Bend radius R (m)	0.0415
Channel hydraulic diameter D_h (m)	0.006
Channel length l (m)	5.22
Working fluid density ρ ($kg \cdot m^{-3}$)	999
Working fluid viscosity μ ($Pa \cdot s$)	0.001

The test rig is customised towards the specific test requirement. As shown in Fig. 2, the fluid inerter is placed in the test rig. The displacement-controlled excitation is generated by the hydraulic actuator (INSTRON DL25kN), which is rigidly connected to a free end of the inerter terminal (cylinder rod). During the tests, the real displacement across inerter terminals is recorded by a suitably placed LVDT (RDP DCTH6000C). Thus, minimum backlash from the joints can be then achieved. The axial force

applied by the fluid inerter is collected using the load cell mounted between the actuator and cylinder rod. Meanwhile, the two pressure gauges are located at both ends of the helical tube to monitor the pressure drops of the fluid during the constant velocity tests. This equipment configuration constitutes the main contribution of the research presented.

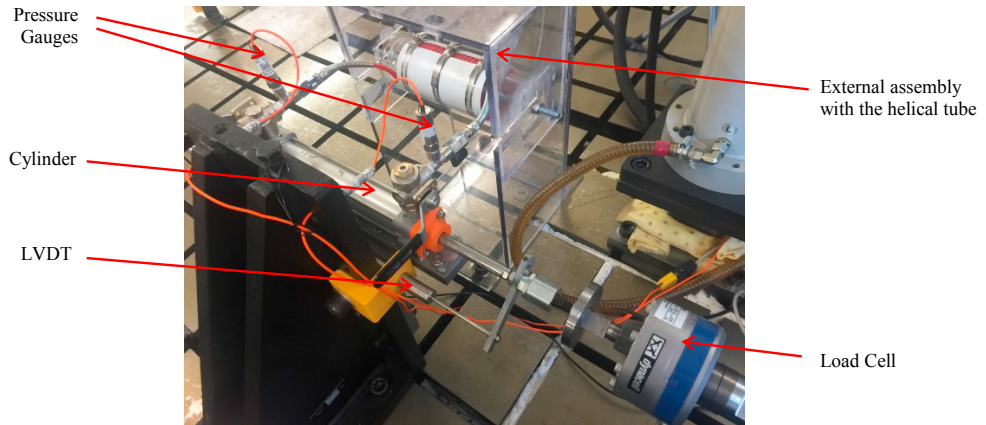


Fig. 2. Test rig for fluid inerter prototypes.

3. Testing and modelling of the damping effects

3.1. Triangular wave excitation tests

In order to test the damping effect separately from other effects such as elasticity and inertance, a triangular wave of the axial displacement is used to excite the free end of the fluid inerter, giving the constant terminal velocities during each direction of the cylinder rod movement. Except for the transition phase after each periodic motion direction change, the steady terminal force is composed of damping and friction only.

The quasi-steady force is dominated by friction at very low velocities (e.g. below 0.01 m/s). Under stated conditions, the damping force is produced by the pressure difference between the two chambers of the cylinder, while the pressure difference results mainly from the fluid viscosity effect in the helical tube channel. Three sets of experimental data are collected during the test, which are the terminal velocities by the LVDT, the terminal forces by the load cell, and the absolute pressures by the pressure gauges.

Since the nonlinear damping through the helical tube requires separate testing at each single terminal velocity, various frequencies of excitation are applied at the constant amplitude. The constant amplitude of 40 mm is chosen because of the resulting longer steady state. Thus, more accurate value of terminal force can be captured. To fully explore the damping properties across wide range of velocities, the tests are carried in the range from 0.0016m/s to 0.224 m/s. The upper limit of the test velocities is restricted by the maximum force supported by the cylinder.

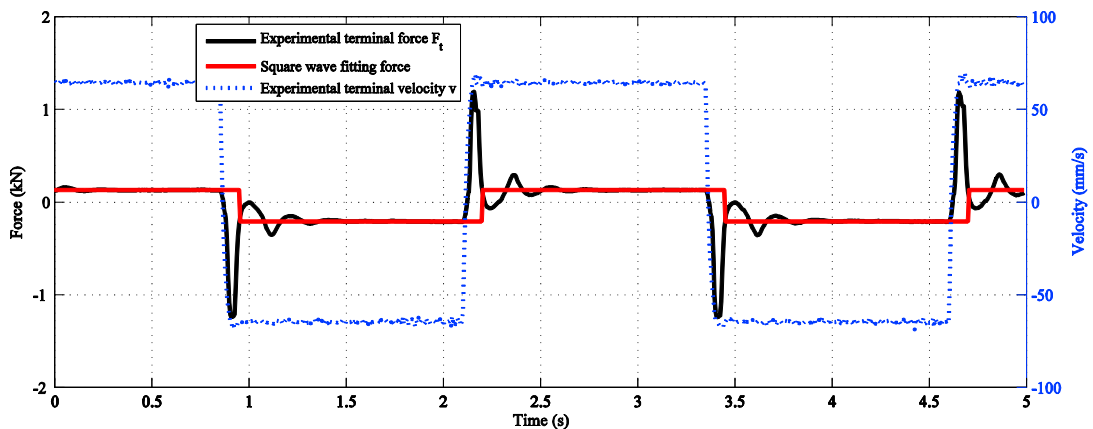


Fig. 3. Square wave fitting to a triangular wave test for the helical-tube fluid inerter.

The method of the least absolute residuals (LAR) [7] is used to fit a curve that minimise the absolute difference of the residuals rather than the squared difference. Therefore, the extreme residual values have less influence on the fitting results. An example of how to identify the damping force from the load cell records is demonstrated in Fig. 3 for the case of the constant terminal velocity of 0.064 m/s. The experimental data are fitted by a square wave with amplitude of 0.1684 kN, which represents the value of steady state terminal force F_t at this velocity. In this case, the extreme values are mainly concentrated in the initial transitional phases. There is an initial offset in the load reading of -0.0357kN, which is removed from the presented readings. Meanwhile, the friction caused by the seals is identified through the low velocity tests, where the terminal force (F_t) is dominated by friction. At the terminal velocity of 0.0016m/s, the identified value of the steady state terminal force is approximate 45N. Hence, the friction force f is estimated to be 45N for this helical-tube fluid inerter.

During the testing at each velocity, two sets of pressure data are collected by the pressure gauges, recording the internal pressure at each end of the helical tube channel. The difference between these two sets of values represents the pressure drop across the helical tube (denoted Δp). As shown in Fig. 4, at the terminal velocity of 0.064 m/s, the pressure drop Δp is identified to be approximate 99000 Pa during the steady state. It is noted that the negative values recorded by the pressure gauges are caused by the initial pressure calibration to be zero for both pressure gauges.

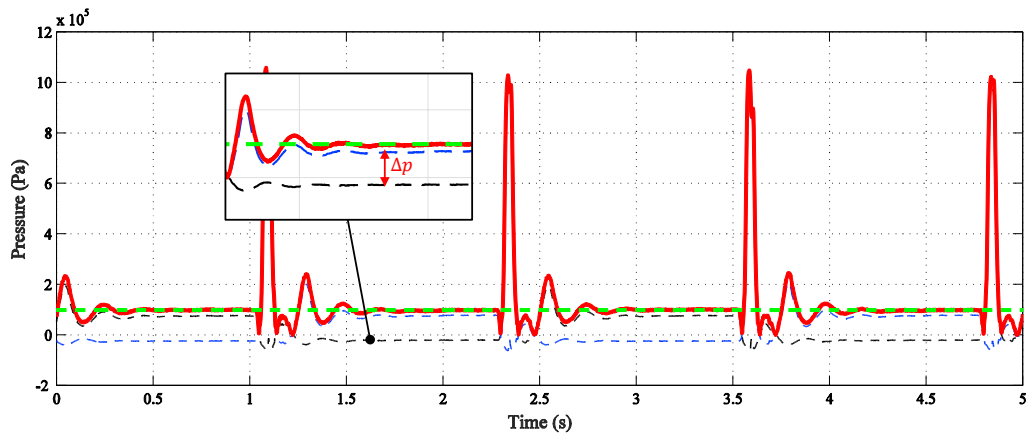


Fig. 4. Pressure drop across the helical tube for strut velocity of 0.064 m/s.

Based on the test results across the full range of terminal velocities, the total damping force (F) is calculated by subtracting friction f from the recorded terminal force F_t at each tested velocity. The total damping force (F) versus terminal velocity (v) for helical-tube fluid inerter is plotted in Fig. 5 by black solid line. In the meantime, the damping force through the helical tube channel is derived by formula $F_h = A_1 \Delta p$, and is also plotted in Fig. 5 as the blue dashed line. The nonlinear damping properties in both cases show the similar trend of more rapid increase in damping when the velocity becomes higher. Furthermore, the total parasitic damping has been shown to be dominated by the helical tube damping due to very small difference between the two sets. The observed discrepancy between these two sets can be explained by the presence of the inlet/outlet damping and potential leakage damping across the cylinder piston.

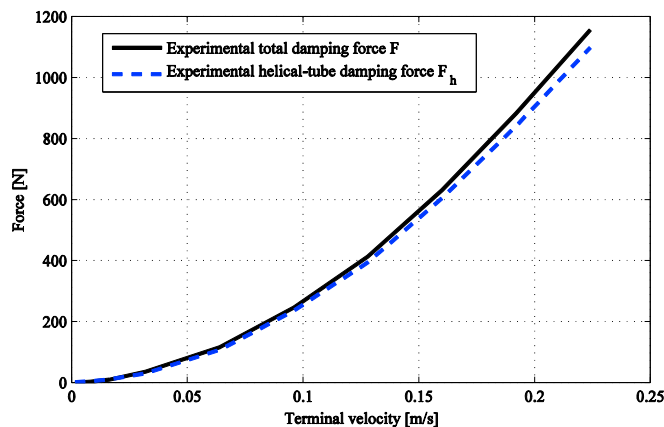


Fig. 5. Total damping force and helical tube damping force versus terminal velocity for the prototype.

3.2. Damping verification and analysis

As shown in the previous section and Fig. 5, the damping through the helical tube channel is the major source of parasitic damping. In order to accurately predict the terminal behavior of a fluid inerter, the theoretical model of the parasitic damping is critically important. There are plenty of experimental and analytical studies aimed at the estimation of the pressure drop due to flow in the helically coiled tubes. Similar to [5], the model introduced by Rodman and Trenc [8] is used for the theoretical helical tube damping (F_h') calculation,

$$F_h' = 0.03426 \frac{2\pi l A_1}{\sqrt{2D_h R}} \left(\frac{A_1}{A_2}\right)^2 v^2 + 17.54 \frac{2\mu l A_1}{D_h^2} \left(\frac{A_1}{A_2}\right) v. \quad (1)$$

According to the parameters in Table 1, the theoretical helical tube damping is calculated by Equation (1) and plotted in Fig. 6(a) by the black dashed line. It is compared with the experimental results shown by the red solid line. In the same way, the theoretical damping and experimental damping for the results from [5] are plotted in Fig. 6(b). It can be seen that the theoretical values fit the experimental result much better for the present study than the study in [5]. The new measuring method is the main reason for improved match between the theoretical and experimental results. However, there is still some discrepancy observed for the high terminal velocities, which could be the raising of fluid temperature, leading to lower density and viscosity of fluid.

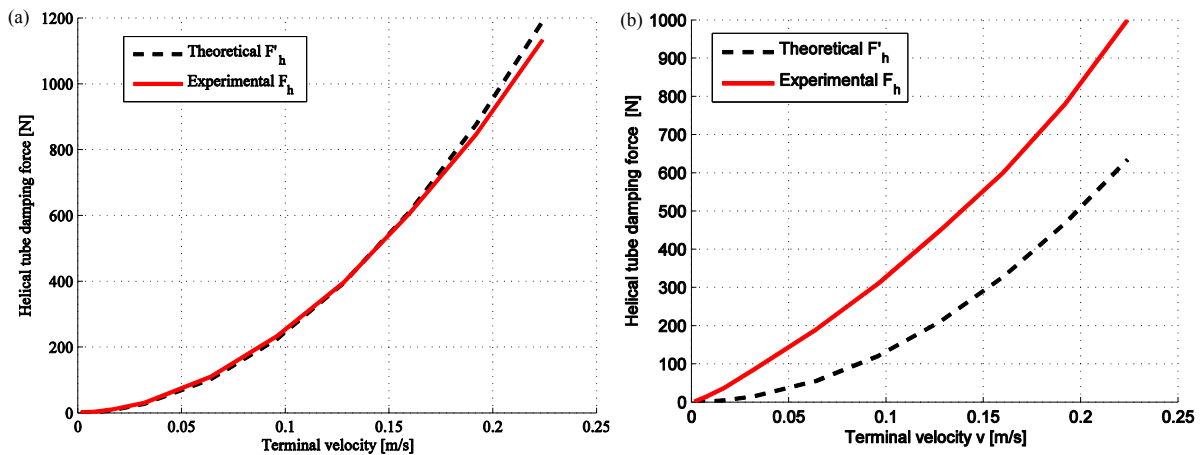


Fig. 6. Comparison between theoretical and experimental helical-tube damping force versus terminal velocity for testing in (a) this study and (b) the study in [5].

4. Design of a meander-tube fluid inerter

A new fluid-based inerter design is proposed with the aim of achieving different damping characteristics, compared to the helical-tube fluid inerter. The meander-tube fluid inerter, as shown in Fig. 7(b), is designed to achieve reduced curved length for a given total length and diameter of tube, while providing similar level of inertance. To verify the potential reduction of damping for the meander-tube design, the total length of the tube is assumed to be the same as for the helical-tube design (see in Fig. 7(a)). The adjacent straight tube parts are tightly packed. Therefore, the bend radius of each U-bend for the meander-tube design is assumed equal to the outer radius of tube, which is approximately 0.004m. Other parameters are the same as for the helical-tube fluid inerter prototype specifications in Table 1.

With the help of Hagen-Poiseuille formula applied for the calculation of the straight tube damping, the theoretical damping through the meander-tube channel is derived by adding the U-bend tube damping, Equations (1) and the straight tube damping,

$$F_m' = N_u \left[0.03426 \frac{2\pi l_u A_1}{\sqrt{2D_h R}} \left(\frac{A_1}{A_2}\right)^2 v^2 + 17.54 \frac{2\mu l_u A_1}{D_h^2} \left(\frac{A_1}{A_2}\right) v \right] + N_s 8\pi \mu l_s \left(\frac{A_1}{A_2}\right)^2 v. \quad (2)$$

where $N_u = 35$ is the number of U-bends and $N_s = 34$ is the number of straight tubes, $l_u = 0.004\pi$ m is the length of each U-bend and $l_s = 0.144$ m is the length of each straight tube

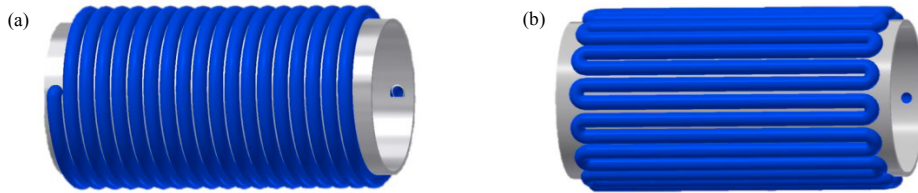


Fig. 7. Fluid inerter external tube configurations of (a) helical arrangement and (b) meander arrangement.

The results of both theoretical damping predictions for the helical-tube arrangement and the meander-tube arrangement are plotted in Fig. 8. It can be seen that the meander-tube design modelled in Equation (2) gives much lower damping over the full velocity range. Based on this result and under the stated assumptions, it can be seen that with the similar dimensions of the device and the same working fluid, the meander-tube fluid inerter should achieve similar inertial effects with lower parasitic damping compared to the original helical-tube design.

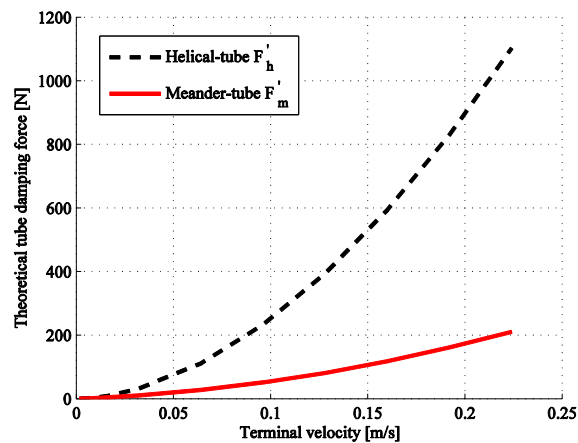


Fig. 8. Theoretical damping of helical-tube and meander-tube fluid inerters.

5. Conclusion

This paper demonstrates a new method for accurate testing of the parasitic damping in the helical-tube fluid inerters based on the use of two pressure gauges at the inlet/outlet of the helical tube. The prototype helical-tube fluid inerter and the customised test rig were built for experimental analysis. The theoretical formula for the nonlinear helical-tube damping has been verified through the comparison with the corresponding experimental data. It can be seen that much better agreement between the theoretical formula and experimental data has been achieved compared with previous studies, because of the improved experimental set-up. In addition, an alternative novel fluid-based inerter design is introduced. The comparison between the theoretical estimates of the helical-tube damping and meander-tube damping serves as the evidence for the potential benefits of this new fluid inerter design.

6. Reference

1. Smith, M.C., *Synthesis of Mechanical Networks: The Inerter*. IEEE Transactions on Automatic Control 2002. 47(10): p. 1648-1662.
2. Papageorgiou, C., Houghton, N.E. and Smith, M.C., *Experimental Testing and Analysis of Inerter Devices*. Journal of Dynamic Systems, Measurement, and Control, 2008. 131(1): p. 011001-011001.
3. Papageorgiou, C. and Smith, M.C., *Laboratory experimental testing of inerters*. in *Proceedings of the 44th IEEE Conference on Decision and Control*. 2005.
4. Fu-Cheng, W. and Wei-Jiun, S., *Inerter Nonlinearities and the Impact on Suspension Control*. in *2008 American Control Conference*. 2008.
5. Swift, S.J., Smith, M.C., Glover, A.R., Papageorgiou, C., Gartner, B. and Houghton, N.E., 2013. Design and modelling of a fluid inerter. *International Journal of Control*, 86(11), pp.2035-2051. *Design and modelling of a fluid inerter*. International Journal of Control, 2013. 86(11): p. 2035-2051.
6. Shen Yujie, C.L., Liu Yanling, Zhang Xiaoliang, Yang Xiaofeng *Optimized modeling and experiment test of a fluid inerter*. Journal of Vibroengineering, 2016. 18(5): p. 2789-2800.
7. Marazzi, A., *Algorithms, routines, and S functions for robust statistics*. 1993, CA: Wadsworth & Brooks/Cole, Pacific Grove.
8. Rodman, S. and Trenc, F., *Pressure drop of laminar oil-flow in curved rectangular channels*. Experimental thermal and fluid science, 2002. 26(1): p. 25-32.